Hydrologic riverbed generation and operational analysis for autonomous vessels in meandering inland waterways

N.B. When citing this work, cite the original published paper.

(article starts on next page)

Hydrologic Riverbed Generation and Operational Analysis for Autonomous Vessels in Meandering Inland Waterways

Chengqian Zhang[a], Jonas W. Ringsberg[a], Fabian Thies[b]*
[a]Division of Marine Technology, Department of Mechanics and Maritime Sciences,
Chalmers University of Technology, Gothenburg, Sweden
[b]FRIENDSHIP SYSTEMS AG, Potsdam, Germany

ABSTRACT

Confined water significantly impacts autonomous vessel navigation. This study introduces a novel method for rapidly generating inland waterway scenarios to validate vessel performance in dynamic confined conditions. A new formula models river hydraulics, incorporating cross-sectional shifts, current fields, deposition, and erosion effects. Validated with U.S. River field data, the formula captures the lateral migration of the thalweg in bends. The hydraulic model was incorporated into a novel voyage planning simulation platform for operational analysis. The ship path following simulations reveal the profound influence of hydrodynamic effects on steering, highlighting the need to integrate bathymetric and current data into control systems to enhance navigational safety for autonomous vessels in confined waterways.

KEY WORDS: Autonomous vessels; control; inland waterways; river hydraulics.

INTRODUCTION

Shifting from road to inland waterways is a promising solution for a sustainable mode of transport by reducing CO_2 emissions (European Environment Agency, 2017). With the increasing degree of autonomy and sensor developments, autonomous inland waterway vessels (AIWVs) are regarded as a key factor in formulating intelligent waterborne transport networks to enhance traffic flow with lower crew and operational costs. Given the distinct nature of inland waterways that channels are constrained by water depth and width, it is particularly important to investigate vessel dynamics and energy consumption to ensure operational safety and efficiency. This requires a voyage planning simulation platform, specifically designed for inland waterways that can capture the physics of vessel behaviour under these meandering rivers.

Simulation platform, such as the development of marine simulators, is a popular research field in the maritime industry. The existing study on simulation platforms are mostly developed for standard commercial vessels in open-sea conditions (Perez et al., 2006; Rutkowski, 2018; Tsou, 2016). The voyage plan is executed and monitored based on a built-in electronic chart display and information system (ECDIS). While these advanced simulation platforms are well-developed for commercial shipping, the majority of them do not consider inland waterways. Navigation in inland water faces unique challenges such as dynamic water depth, narrow channel width, and the presence of artificial infrastructures (Norrbin, 1976; Vantorre et al., 2003). Vessels will be subject to additional hydrodynamic loads from shallow water and channel banks, which might affect their manoeuvrability. Besides, inland vessels are significantly influenced by various hydrological factors, including water currents, shape and curvature of the river channel, and changes in riverbed and morphology. Therefore, the voyage should be carefully examined by simulating the vessel performance under these effects since the operational space is fairly constrained in inland waterways. Nevertheless, the hydrodynamic impact, as well as the hydraulics features of rivers, are normally oversimplified or even neglected in most of those existing simulators.

The inland ECDIS is relatively new and has been continuously developed during the past decades (CCNR, 2014). However, extracting detailed river profile information is often challenging as ECDIS normally comes integrated into built-in software. Moreover, these commercial simulators are typically complex and contain massive features, making them less applicable for research purposes. Hence, the aim of this study is to develop a holistic simulation platform. Hence, this study aims to develop a modular-based and efficient simulation platform specifically designed for AIWVs. This platform offers a holistic approach, enabling the evaluation of vessel performance from early design to operational stages. A key feature of the proposed platform is the incorporation of a novel hydraulic model, allowing for the rapid generation of arbitrary inland waterways for simulation analysis. By integrating manoeuvring, control and energy system performance models, this platform enables the simulation of AIWVs' navigation performance in various inland waterways and provides rapid energy consumption predictions.

HYDROLIC MODELLING

Hydraulic model is a critical factor for analysing the vessel dynamics, especially in confined inland waterways. These models represent key features such as bathymetry profiles, channel geometry, and current fields along meandering waterways, which are essential for vessel handling (manoeuvring) and control design. Most present study focuses on developing sophisticated control method while the waterway itself is normally over-simplified, e.g. based on straight or other simple channel shapes with constant water depth. Therefore, the hydraulic model in this study is presented into two phases: (a) waterway generation, which facilitates the creation of arbitrary meandering channels, and (b) cross-sectional modelling, which presents a novel formula for capturing cross-sectional shifts.

Waterway generation

An arbitrary meandering river can be generated by using a combination of straight and curved sections with varying size (Fossen, 2011; Paulig & Okhrin, 2024). This study follows this method for waterway generation, as shown in Fig. 1. The waterway is constructed using a series of straight and curved segments $(S_1, S_2, ..., S_i)$. Each segment is further divided into a set of cross-sections $c_{i,j}$ by evenly distributed grid points according to its geometry. The rivers generated are assumed to have a constant width, represented by 15 grid points in the transverse direction, with a spacing of 15 m between adjacent points, resulting in a total width of 225 m.

Straight segments are defined by a parameter controlling their segment length, except for the first segment, which also includes an arbitrary starting angle. Curved segments are generated according to two random variables: the radius r_i and the segmental angle θ_i. It should be noted that each new segment is transformed to properly attach and align with the ending cross-section of the previous segment, maintaining continuity and geometric consistency.
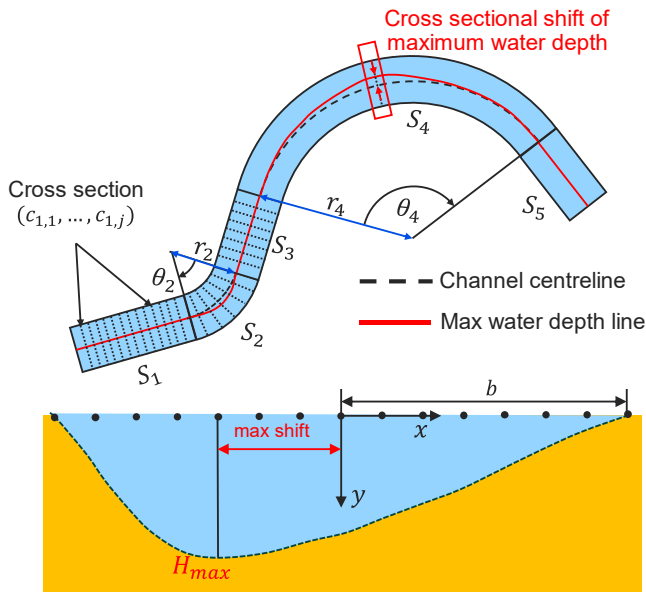

Fig. 1 Schematics of meandering waterway generation and cross-sectional shift modelling.

Cross-section modelling

In the existing research, the shape of river cross-section is normally simplified into rectangular or trapezoidal. Most recent study can be found in Paulig and Okhrin (2024), where the shape function of channel cross-section is modelled using a normal distribution liked formula. However, the maximum depth is assumed locate always in river centre, meaning that the shifting of riverbed in curved segmented is neglected. Besides, the current filed did not include the impact of bathymetry and waterway geometry.

To capture the characteristics of natural inland waterways, this paper proposes a new formula to model the hydrological change of cross-sections. The depth profile is modelled using the equation below:

$$h_{i,j} = (1 + \varepsilon_h) \cdot H_{max} \cdot \left(\frac{y}{\min(y)} \right) \tag{1}$$

where $h_{i,j}$ represent water depth of cross-section j along the ith segment, ε_h is a random perturbation in normal distribution with a standard deviation of 0.1, H_{max} is the maximum depth of the cross-section, y represent the shape function of the riverbed, calculated using the equation:

$$y = -\left(1 - \left(\frac{x}{b}\right)^2\right) \cdot \left(1 + \gamma_{i,j} \cdot \left(\frac{x}{b}\right)\right) \tag{2}$$

where x is the lateral position, b is the half width of the channel, and $\gamma_{i,j}$ is a skewness factor which calculates the cross-sectional shifts depending on the shape of the waterway. This is given as:

$$\gamma_{i,j} = \alpha \cdot \left(\frac{\theta_i}{max(\theta)} \right) \cdot \left(1 - \left(\frac{\Delta i, j}{(r_i \cdot \theta_i)/2} \right)^2 \right) \tag{3}$$

where α is a constant to decide the direction segment curvature $\alpha \in [-1, 0, 1]$, meaning that the skewness is 0 for straight segment, and being negative if the curvature towards left, and vice versa, θ_i is the angle of the segment, $\Delta i, j$ is arc distance between cross-section j and the mid-section within this segment (as shown in red box), and r_i is the radius of the segment, as shown in Fig. 1. The equation above assumes that the maximum shift is located in the middle of a curved segment.

Current field

As suggested by Odgaard (1989), in river meaner the distribution of stream velocity in transverse direction generally complies with its corresponding water depth. Therefore, the current field generation follows a similar process in the previous section. The equation of current velocity is

$$u_{c_{i,j}} = (1 + \varepsilon_c) \cdot u_{max} \cdot \frac{\left(-\left(1 - \left(\frac{x}{b}\right)^2\right) \cdot \left(1 + \gamma_{i,j} \cdot \left(\frac{x}{b}\right)\right) \right)}{\min(y)} \tag{4}$$

where U_{max} is the maximum flow velocity, ε_c is the disturbance to include uncertainties of flow speed. It can be found from the equation that, the current speed distribution along the transvers direction is near parabolic shaped in straight segments, and in curved segments the maximum flow speed is located based on the shifting of the depth profile. Moreover, it should be noted that the flow direction is perpendicular to each cross-section. Meaning that the vortex flow or secondary flows cannot be modelled, and they are thus neglected.

VOYAGE PLANNING PLATFORM

This section presents the development of a voyage planning platform specifically designed to AIWVs. The model is modular and is designed to rapidly predict energy consumption during ship navigation by integrating key factors such as hydrodynamics, manoeuvrability, bathymetry, and control algorithms, as shown in Fig. 2. The primary goal of this platform is to provide a holistic system for assessing the performance of a virtual AIWV under dynamic conditions. This system encompasses the following components:

1. A ship design model, which formulating the speed-power relationship of inland vessel based on loading, resistance and propulsion.
2. A manoeuvring model that calculates rigid body vessel dynamics under confined inland water.
3. A control model, designed for heading and speed control to ensure path following.
4. A hydraulic model, capable of generating arbitrary river meanders, including current and depth profiles.

With these models, a voyage planner is developed for operational analysis. The outcome is mainly divided into two-fold: (a) vessel trajectories and navigable zones, and (b) dynamic feedback of power demand and energy consumption based on the encountered waterway conditions.
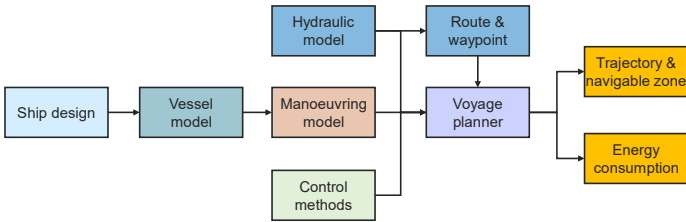

Fig. 2. Structure of the voyage planning platform for AIWVs.

Ship energy performance modelling

The primary function of the ship performance model is to provide rapid feedback on energy consumption by formulating the speed-power relationship. Such a model is important for autonomous systems, as it enables the monitoring of dynamic energy demand during navigation— a prerequisite for the optimal utilisation of fuel or electricity. Nevertheless, it is challenging to predict the energy consumption of autonomous vessels, especially in the early design stage since the available information and parameters are very limited. In our previous study (Zhang et al., 2023), a physics-based ship performance model, ShipCLEAN-IWV, was developed to establish the energy system of inland vessels, as shown in Fig. 3. This model consists of pure empirical and analytical methods. The resistance prediction includes a modified formula to account for shallow-water and bank impact from inland water. Following by ducted-propeller design, and engine modelling, the total fuel consumption can be calculated using equation:

$$FC = SFOC(0.5\rho_{FW}S_W C_T V_S^2 + R_S + R_{BANK})V_S/\eta_H/\eta_O/\eta_R/\eta_S \quad (5)$$

where the specifical fuel oil consumption ($SFOC$) rate is derived from a regression method (Hidouche et al., 2015), ρ_{FW} is the fresh water density, S_W is the wetted surface area, C_T is the total resistance coefficient in deepwater, R_S is shallow water resistance, and R_{BANK} is bank induced resistance, V_S is the vessel speed, η_H is the hull coefficient, η_O is propeller open water coefficient, η_R is the relative rotative efficiency, and η_S is the shaft transmission efficiency, detailed parameters can be found in Zhang et al. (2023).
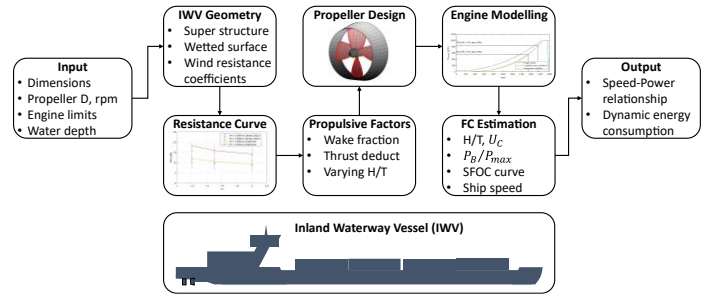

Fig. 3. Overview of ShipCLEAN-IWV model, reproduced from Zhang et al. (2023).

Manoeuvring and control

The manoeuvring model is another critical component of the voyage planning system, as accurate and dynamic updates of vessel motion are essential during navigation. Inland vessels are typically equipped with twin propellers and multiple rudders to ensure adequate manoeuvrability in confined waterways. The coordinate systems used in this study are illustrated in Fig. 4. It is important to note that only two-dimensional (2D) planar ship motion (surge, sway and yaw) is considered, as inland vessels typically operate in calm water where vertical motion can be neglected. In the coordinate systems, $o_0 - x_0 y_0 z_0$ is the earth-fixed frame, $o - xyz$ is the body-fixed frame locate in midship, G is the centre of gravity (CoG), u and v denote the surge and sway speed, respectively.
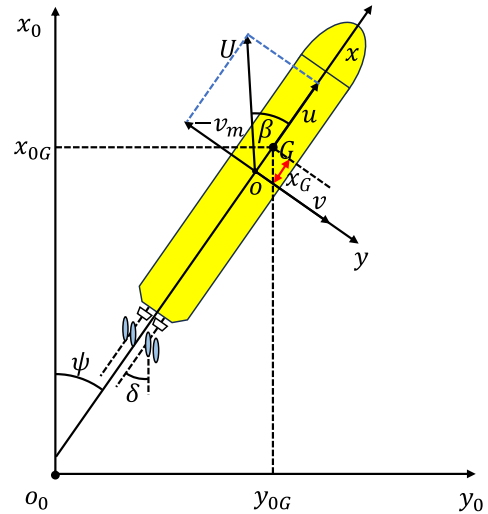

Fig. 4. Coordinate system of inland vessel with twin propeller multiple rudder configuration.

Most existing studies on ship manoeuvring focus on conventional commercial vessels. These manoeuvring models are typically developed for open water conditions, which may not be directly applicable to inland waterways, as these channels are often constrained by limited width and shallow water depth. Therefore, this study adopts a modified version of manoeuvring modelling group (MMG) model with shallow water and bank effect (Zhang et al., 2024). The equation of motion is given as:

$$\left.\begin{array}{l}(m+m_x)\dot{u} - (m + m_y)v_m r - x_G m r^2 = X_H + X_P + X_R + X_B \\ (m+m_x)\dot{v}_m - (m+m_x)ur + x_G m\dot{r} = Y_H + Y_R + Y_B \\ (I_z+x_G^2 m+J_z)\dot{r} + x_G m(\dot{v}_m+ur) = N_H + N_R + N_B\end{array}\right\} \quad (6)$$

where the left side shows the mass m and inertia terms I_z, m_x and m_y represent added mass in the corresponding direction, v_m is the sway speed at mid-ship, r is the yaw rate. The right side denote force and moment acting on the ship from different parts, the sub script H, P, R, and B means load from hull, propeller, rudder and bank effect. It is important to note that shallow water effect is included in the hull force by a correction of resistance coefficient and hydrodynamic derivatives. The bank-induced force and bow-out moment are modelled using an average value of three methods (Ch'Ng et al., 1993; Norrbin, 1976; Vantorre et al., 2003).

Guidance navigation and control

AIWVs require precise control systems to ensure operational safety, as they frequently navigate in confined waterways. In addition to shallow water conditions, river currents can significantly impact course stability. Therefore, the design of the Guidance, Navigation, and Control (GNC) module in this study accounts for these disturbances. The primary objective is to execute effective rudder control to maintain the vessel's heading along predefined waypoints while minimizing cross-track error (XTE). The demonstration of the GNC module is shown in Fig. 5. The heading control is implemented based on the Line of Sight (LOS) scheme, where the desired heading angle is calculated from the current position and heading. The desired heading angle is determined using the following equation:

$$\psi^{ref} = \psi_{WPT} + \psi_{cross} - \beta \qquad (7)$$

where ψ_{WPT} is the angle between the next and current waypoint as guidance from course, ψ_{cross} is the angle to offset the cross-track error by including an advance distance X_D. The control design adopts a proportional-integral-derivative (PID) controller to update the rudder angle δ_c, the equation is:

$$\delta_c(t) = K_p \left(\psi_e(t) + T_d \big(\psi_e(t) - \psi_e(t-1) \big) + \frac{1}{T_i} \left(\sum_{l=0}^{t} \psi_{e_l} \right) \right) \qquad (8)$$

where $\psi_e(t)$ represents the heading error at the current time step t, K_p is the controller's proportional gain, and T_d and T_i are the derivative and integral time constants, respectively.
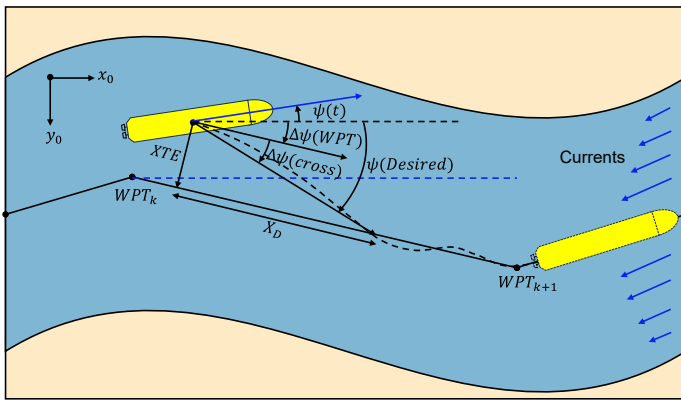

Fig. 5. Heading control under river current.

RESULTS

This section presents the simulation results from the voyage planning system. First, a validation study of cross-sectional modelling is conducted using field measurements of river bathymetry data.

Subsequently, route planning and control simulations are carried out to evaluate the operational performance of the AIWV under various inland waterway scenarios.

Bathymetry Prediction and Validation

It is important to ensure that the propose hydrological formula can capture the cross-sectional shift of river meanders. Hence, this formula is validated using real field measurements taken at the confluence of the Wabash and Embarras Rivers in the United States. (Parsons et al., 2013). The multibeam bathymetry data is shown in Fig. 6, and cross-section 4 is selected as an example for maximum depth shift analysis. It should be noted that, this cross-section is located relatively in the middle of the curved river, where a significant depth profile shifting towards outer bank is observed, as shown in the figure. Therefore, the skewness factor in Eq. 3 is assumed to be 1 for prediction. Then the remaining parameters are the maximum cross-sectional water depth H_{max} and the channel width $2b$. As shown in the depth profile, the H_{max} is 12 m, and the river width is 140 meters approximately instead of 125 m in transversal direction. The discrepancy arises because the sonar measurements have gaps near each side of the banks, which is also the reason the measured depth did not start with 0 m, as seen in Fig. 6.

The cross-section can be predicted based on these parameters, and the result is shown Fig. 7. The results demonstrate that the proposed equation accurately predicts the trend of cross-sectional shifting. The location of the maximum water depth aligns well with the measurements. Deviations can be also noticed especially in the inner (left) bank, but accurately predicting the deformation of riverbed slopes is normally very challenging, as it involves complex river hydrodynamics and sediment transport modelling. The primary objective of this formula is to provide a fast and efficient method for capturing the general shifting of cross-sections in river meanders.
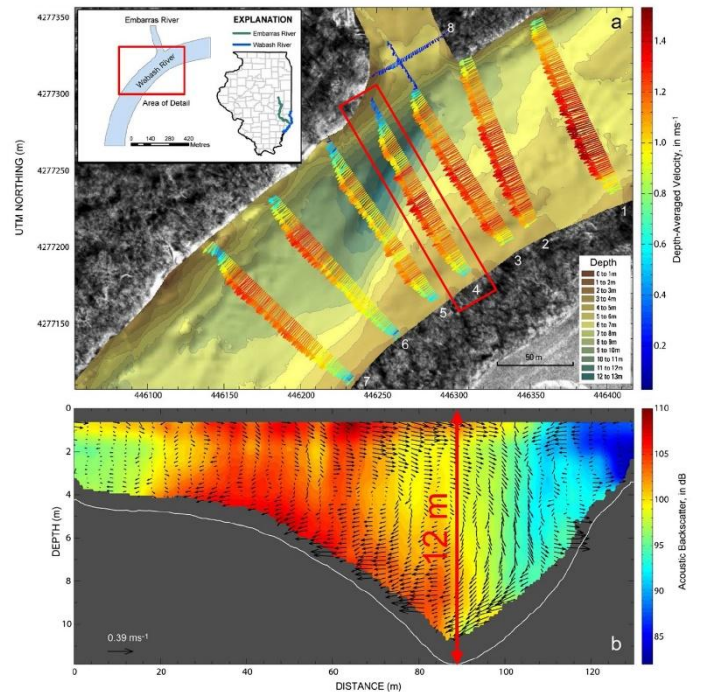

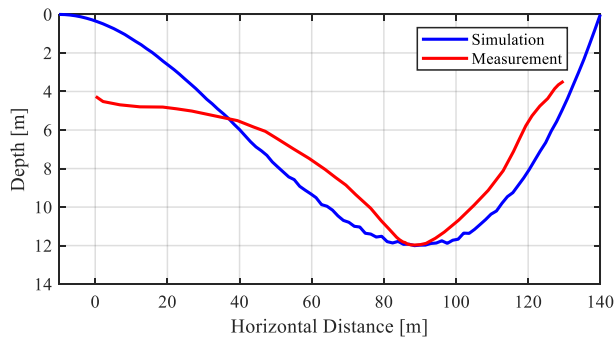Fig. 6. Field measurements of Wabash River (Parsons et al., 2013).

Fig. 7. Bathymetry profile and simulation results of cross-section 4.

Waterway generation

Arbitrary-shaped inland waterways can be generated by using a series of straight and curved segments using the hydraulic model. An example river section with a length of 10 km is showcased in Fig. 8, where this section is constructed using 20 individual segments, including 10 straight ones lengthening randomly between (300 and 600) m and other ten curved segments with a radius ranging from 300 to 500 m and angles between $30°$ to $90°$. The H_{max} value varies at each cross-section following a normal distribution $N(9, 0.3^2)$. It can be clearly seen from the colour map that, in straight segments, the maximum water depth follows the river centre, while significant shifting of the maximum water depth is observed at sharp bends, e.g. at bends 4, 6 and 9 (highlighted in red text).
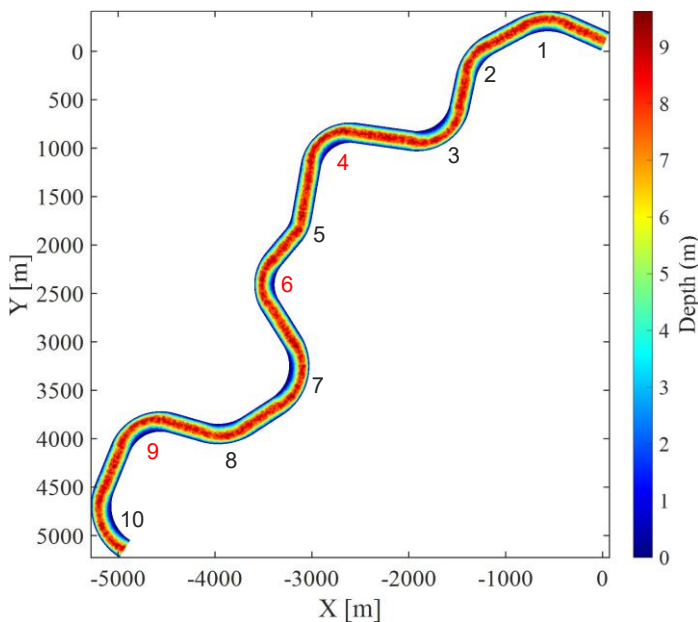

Fig. 8. An example of a generated waterway with depth profile.

Voyage simulation and operational analysis

Vessel profile

A classic pusher-barge convoy is used in this study as the base model to represent a typical type of autonomous inland vessels. The convoy consists of one pusher boat and one rake barge to formulate the 11BP system. The convoy equipped with a steering system including twin propeller and four rudders. The main dimensions, propeller, and rudder

profile of the convoy are listed in Table 1. The hydrodynamic derivatives of the pusher-barge model are taken from the model test conducted under three water depth to draught ratios (H/T): 19.3 for deep water, 1.5 for medium shallow water, and 1.2 for shallow water. These coefficients are detailed in Koh and Yasukawa (2012). During simulations, the hydrodynamic derivatives are interpolated based on the current water depth using regression results. To prevent incorrect extrapolations, the minimum water depth is constrained to $H/T = 1.2$ if it falls below this value.

Table 1. Dimensions and profile of propeller and rudder

Parameters	Pusher	Rake-barge	Convoy
Length, L [m]	40.00	60.96	100.96
Ship Beam, B [m]	9.00	10.67	10.67
Draught, T [m]	2.20	2.74	2.74
Displacement, ∇ [m³]	494.7	1646.2	2140.9
Block coefficient, C_B [-]	0.633	0.924	0.725
Propeller and rudder configuration			
Propeller diameter, D_P [m]	1.8		
Revolution speed, n_P [rpm]	300		
Rudder span, B_R [m]	2.0		
Rudder chord length, C_R [m]	2.0		
Rudder area, A_R [m²]	4.0		

Case 1: sailing along channel centre

The first scenario of voyage planning for AWIVs is river centre navigation, which is a very typical condition when the waterway is clear. If the traffic condition allows, sailing at river centre helps avoid shallow water regions and minimises disturbances from bank effect. In this scenario, the vessel keeps a constant 80% engine load with a fixed propeller speed of 250 rpm while navigating under upstream current with u_{max} of 1.2 m/s. Fig. 9 presents the simulation results, showing that the vessel follows the desired track well, particularly at straight segment, as demonstrated in the blue box. At river bends, the vessel trajectory shows some deviations due to disturbance from the current and the inherent delay from the vessel's turning response. Despite these deviations, the overall tracking performance demonstrates the effectiveness of the control design under this scenario.
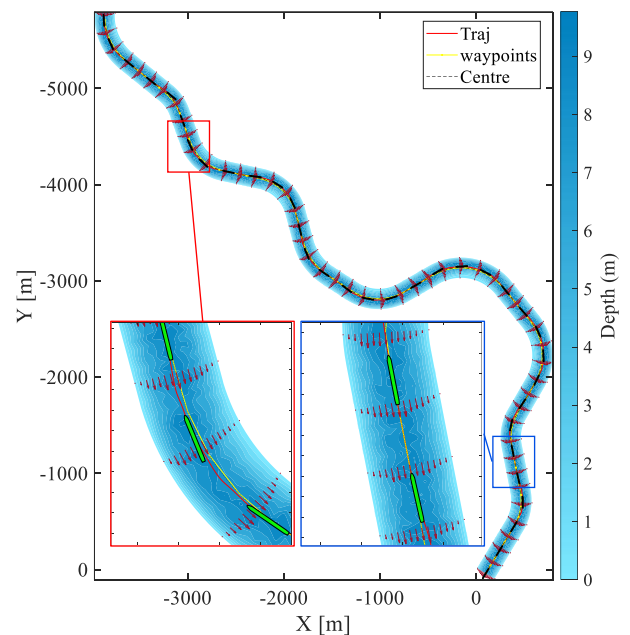

Fig. 9. Trajectory of navigation along the river centre.

3104

Case 2: bridge passing and stopping test at lock

In inland waterways, the presence of many artificial infrastructures, such as bridges and locks, makes the manoeuvring and control design should be carefully investigated since the operational space is significantly confined by these structures. Hence, the simulation presented in this subsection is aiming at evaluating the performance of the voyage planning system under scenarios involving bridge pillars and locks. The vessel maintains a constant propulsion speed until it approaches a bridge pillar or lock. When approaching these structures, the propeller speed must be reduced and, if necessary, reversed to stop the vessel successfully. The range is selected by the distance head S_d between vessel to these structures, given as:

$$n = \begin{cases} 0.5n_{max}, & S_d \ll 2L \quad (bridge\ passing) \\ -0.5n_{max}, & S_d \ll 3L \quad (lock\ stopping) \end{cases} \quad (9)$$

The equation above indicates that when the ship approaches a bridge within a distance of less than twice the ship's length, the propeller load is reduced to 50% to ensure safe passage. Additionally, the propeller needs to rotate astern to stop the ship when nearing river locks. Based on this configuration, the simulation results are presented in Fig. 10. In this scenario, the bridge is positioned in the middle of the river segment, which has an overall channel width of 225 m. The span between each bridge pier is 30 m. The river lock, located at the upper right part of the map, consists of two chambers designed to facilitate vessel passage through in double-lane.

The aim of this simulation is to test the performance of the voyage planner under highly restricted conditions. From the results shown in the figure, it can be concluded that the vessel successfully follows the desired route, even under disturbances caused by river banks. The blue bounding box highlights the vessel's ability to safely pass through the bridge with reduced RPM. The heading angle aligns well with the route, and no significant drifting is observed during this manoeuvre. When the vessel approaches the lock, the propeller starts to rotate astern, effectively making the vessel stop within the lock chamber, as indicated by the red bounding box. This can be also reflected in the speed plot, as shown in Fig. 11. The vessel keeps a relatively constant speed for most of the time, with noticeable speed reductions when approaching the bridge and the lock. It is important to note that the vessel is considered fully stopped when its speed drops below 0.05 m/s.
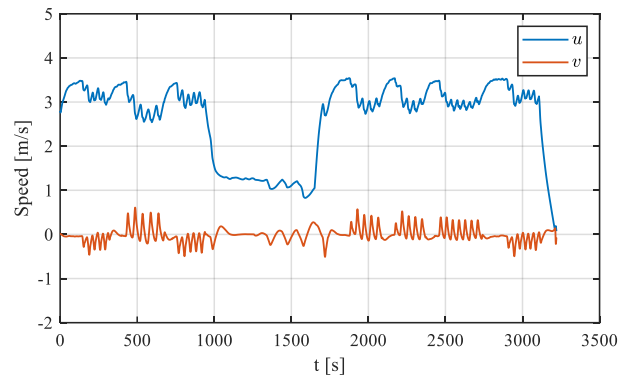

Fig. 10. Simulation for bridge passing and lock stopping test.

Fig. 11. Time histories of surge and sway speed.

Case 3: speed reduction simulation

From the simulations presented in previous cases, it can be notice that course deviations occur during vessel turns due to the constant RPM maintained throughout navigation. Therefore, in this case, the tracking performance is further analysed by implementing speed reduction based on the angle between upcoming waypoints, as shown in Fig. 12, the route deviation is determined using three consecutive waypoints, and the corresponding RPM range is selected according to Table 4. The analysis reveals that if the angle is relatively small, the route is considered as a straight course, and no speed reduction is needed. As the angle increases, the speed should be reduced accordingly. Speed reduction is necessary when vessel need to perform tight manoeuvres on sharp river bends while also saving energy since there is no benefit to operate with a high rpm under large drifting angles.
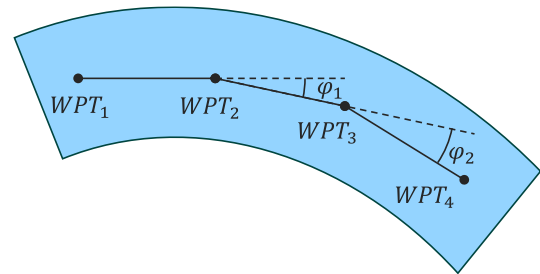

Fig. 12 Waypoint angle for speed reduction.

Table 2. Speed range based on route deviation.

φ (deg)	Rpm [%]
0-5	100
5-10	90
10-15	75
15-20	60
>20	45

The simulation result is shown in Fig. 13. Notably, the zoomed-in path illustrates that by adapting speed reductions, the vessel trajectory (blue dashed line) showcases fewer deviations from the waypoints compared to the trajectory operating with constant RPM. Reducing the speed provides sufficient operational time for effective manoeuvring around river bends, thereby enhancing the tracking accuracy.

Considering the inherent delay in the vessel's turning response, these deviations can be further minimised by pro-active rudder actions. Achieving this would require accurate calculations of advanced distances under different speeds and rudder angles to compensate vessel's turning behaviour effectively.
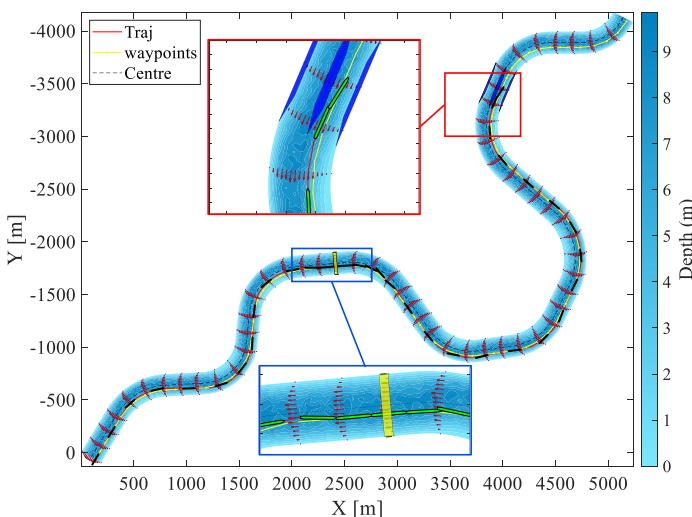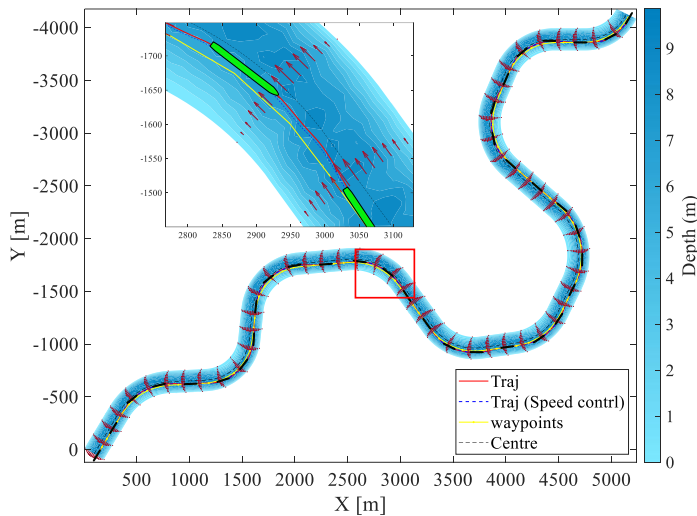
3105

Fig. 13. Vessel trajectories with (blue line) and without (red line) speed reduction.

Based on the dynamic power calculated at each time step, the total energy consumption is estimated through the regression model presented in Hidouche et al. (2015). This model was derived from measurements provided by various marine diesel engine suppliers across a range of power outputs, and the detail of the model is partially shown in Table 3, where the engine load X is defined as the ratio of dynamic engine power at each time step over the engine limit. Using this approach, the total energy consumption under different operational modes and current directions is listed in Table 4. It is important to note that significant energy consumption reduction can be achieved via speed control, with fuel savings of 26.9% and 32.4% observed for upstream and downstream navigation, respectively. These results highlight the potential of optimised speed management in reducing operational energy demands.

Table 3. Engine regression model.

P_{max} [kW]	X [%]	$SFOC = f(X)$ [g/kW/h]	Error [%]
100–300	0–20	$398.89X^{-0.1987} + 8.945$	10
	20–100	$242.51 - 0.810X + 0.0065X^2$	7
300–500	0–20	$342.077X^{-0.1361}$	10
	20–100	$237.84 - 0.5957X + 0.0040X^2$	7
500–1000	0–20	$327.708X^{-0.1262} + 1.984$	15
	20–100	$230.192 - 0.4496X + 0.0033X^2$	10
1000–2000	0–20	$296.346X^{-0.0963} - 1.06$	10
	20–100	$236.786 - 0.7577X + 0.0064X^2$	10

Nevertheless, such significant fuel saving is achieved also by sacrificing the sailing time. The results indicate that the total voyage time with speed control is noticeably longer compared to maintaining a constant RPM. Therefore, future work should focus on conducting energy optimisation analyses under time constraints, where engine speed optimisation is performed to achieve a fixed estimated time of arrival (ETA). Additionally, the performance of various optimisation algorithms should be evaluated using two key metrics: fuel-saving percentages and course deviations (cross-track errors). This approach will ensure energy efficiency while maintaining precise navigations.

Table 4. Energy consumption analysis including speed reduction

rpm	Direction	Distance (m)	Time (s)	FC (kg)
250	Upstream	10033.73	3244	218.48
Speed control	Upstream	10026.10	4879	159.52
250	Downstream	10103.88	2156	145.86
Speed control	Downstream	10088.86	2568	98.56

CONCLUSIONS

This paper presented the development of a novel voyage planning system specifically designed for inland waterway transport. The platform provides rapid predictions of autonomous inland vessels' performance, spanning from ship design to dynamic operational analysis.

The voyage planner includes a new hydraulic model that enables rapid generation of river segments while accurately capturing the bathymetry profiles of natural river meanders. This model was validated against field measurements from a river confluence in the United States. The results demonstrate that the proposed formula correctly modelled the cross-sectional shift based on the position of the inner and the outer banks in the river bends.

Simulations were conducted across different operational scenarios to evaluate the system's tracking performance. These included river centre navigation and near-bank sailing. The results confirm the effectiveness of the control design, enabling the vessel to follow the desired path under various disturbances such as shallow water, currents, and bank effects. Additionally, bridge-passing and lock-stopping tests demonstrated the platform's capability to navigate vessels in highly confined waterways.

Lastly, an energy consumption analysis was performed using a speed reduction scheme based on route deviations. The findings highlight the necessity of dynamically adjusting engine speeds according to waterway conditions to optimise energy efficiency. Future work will focus on investigating energy consumption reduction using various optimisation algorithms under fixed ETA constraints, ensuring a balance between energy savings and operational efficiency. In addition, different steering systems, such as azimuth thrusters, will be compared and evaluated based on their manoeuvrability and tracking performance.

ACKNOWLEDGEMENTS

REFERENCES

CCNR. (2014). *Leaflet on Inland ECDIS*. https://www.ccr-zkr.org/files/documents/ris/leafecdis2014_e.pdf

Ch'Ng, P., Doctors, L., & Renilson, M. (1993). "A method of calculating the ship-bank interaction forces and moments in restricted water,"

European Environment Agency. (2017). *Specific CO2 emissions per tonne-km and per mode of transport in Europe*. https://www.eea.europa.eu/data-and-maps/daviz/specific-co2-emissions-per-tonne-2#tab-chart_1

Fossen, T. I. (2011). *Handbook of marine craft hydrodynamics and motion control*, John Wiley & Sons.

Hidouche, S., Guitteyn, M., Linde, F., & Sergent, P. (2015). "Ships propulsion: estimation of specific fuel consumption based on power load factor ratio," *Proc., Hydrodynamics and simulation applied to inland waterways and port approaches. SHF, Société hydrotechnique de France*,

Koh, K., & Yasukawa, H. (2012). "Comparison study of a pusher–barge system in shallow water, medium shallow water and deep water conditions," *Ocean Engineering*, 46(9-17.

Norrbin, N. H. (1976). "Bank effects on a ship moving through a short dredged channel," *Naval Hydrodynamics Series*,

Odgaard, A. J. (1989). "River-meander model. I: Development," *Journal of Hydraulic Engineering*, 115(11), 1433-1450.

Parsons, D. R., Jackson, P., Czuba, J. A., Engel, F., Rhoads, B. L., Oberg, K., Best, J. L., Mueller, D., Johnson, K., & Riley, J. (2013). "Velocity Mapping Toolbox (VMT): A processing and visualization suite for moving-vessel ADCP measurements," *Earth Surface Processes and Landforms*, 38(11), 1244-1260.

Paulig, N., & Okhrin, O. (2024). "Robust path following on rivers using bootstrapped reinforcement learning," *Ocean Engineering*, 298(117207.

Perez, T., Smogeli, O., Fossen, T., & Sorensen, A. J. (2006). "An overview of the marine systems simulator (MSS): A simulink toolbox for marine control systems," *Modeling, identification and Control*, 27(4), 259-275.

Rutkowski, G. (2018). "ECDIS limitations, data reliability, alarm management and safety settings recommended for passage planning and route monitoring on VLCC tankers," *TransNav: International Journal on Marine Navigation and Safety of Sea Transportation*, 12(3),

Tsou, M.-C. (2016). "Multi-target collision avoidance route planning under an ECDIS framework," *Ocean Engineering*, 121(268-278.

Vantorre, M., Delefortrie, G., Eloot, K., & Laforce, E. (2003). "Experimental investigation of ship-bank interaction forces,"

Zhang, C., Ma, Y., Thies, F., Ringsberg, J. W., & Xing, Y. (2024). "Towards autonomous inland shipping: a manoeuvring model in confined waterways," *Ships and Offshore Structures*, 1-13.

Zhang, C., Ringsberg, J. W., & Thies, F. (2023). "Development of a ship performance model for power estimation of inland waterway vessels," *Ocean Engineering*, 287(115731.